Rainfall induced deformations of road embankments

Edoardo E. Alonso*, Antonio Lloret*, Enrique Romero*

Summary

The paper describes erosion, shallow instabilities and fill collapse induced by heavy rainfalls in several road embankments. Collapse oedometer and suction controlled shear tests were performed on samples recovered in borings. A coupled unsaturated flow-deformation analysis has been carried out to investigate the risk of future failures and the remaining collapse potential of the fill in case of further heavy rains.

1. Introduction

In October 1994, heavy rainfalls affected several embankments of a new road built in Northeastern Spain. Fig. 1 shows the rain distribution during the months of September and October. Most of the damage developed during two days of extremely intense rain (122.8 l/m^2 and 56.5 l/m^2 respectively). The observed damage included extensive erosion of slopes, which in several points undermined the pavement structure, instability of foundation footings for traffic signals and display frames, gaps opened between bridge abutments and fills, translational shallow slides which badly destroyed the top layer in which an incipient vegetation was growing and, more importantly, the development of extense voids below transition slabs connecting earth fills and bridge abutments. This latter case is illustrated in the scheme given in Fig. 2.

Immediately after the events, an investigation was set out in order to establish the reasons for the distress observed and to relate it to the properties and construction method used. It was also desired to know if further damage could ensue as a result of further extreme rainfall and the precautions which should be adopted for the future. This paper gives an account of the investigations and analysis carried out and highlights some conclusions which may be of general applicability.

2. Properties of compacted soil

Low plasticity sandy clays, which are residual granitic soils, were used to build the embankments.

* Universitat Politècnica de Catalunya, Barcelona, Spain

Normal Proctor compaction conditions provided the reference condition to perform the quality control. Dry density and water content were measured by means of a nuclear probe. Acceptance or rejection of a layer was solely based on the dry density reached during compaction. The average measured dry density was 1.85, slightly in excess of the average Normal Proctor value. However, compaction water content consistently remained 2% to 5% below optimum. Its average value was 9.4%.

After the rains, undisturbed samples were recovered in several borings located either at the center or at the edge of the embankment cross section. Identification, oedometer and suction controlled shear tests were performed on some samples. The main results are reported below.

2.1. Identification tests

Some of the samples tested (two out of sixteen) were found "non plastic" but, in general, the soil was classified as a silty or low plasticity clay with liquid limits in the range 31%-46% and plasticity indexes in the range 21%-26%. The average water content was 13.2% (6%-18%), a figure which should be compared with the average water content measured during construction (9,3%). Average dry unit weight (1.758 T/m^3) was however closer to the average value determined during construction (1.85 T/m^3).

Measured values of degree of saturation have been plotted in Fig. 3 as a function of depth. No clear trends are defined but it is apparent that the fills remained unsaturated after rainfall. The average degree of saturation is close to 0.75.

2.2. Wetting under load tests

The remaining collapse potential of the compacted fill was investigated by means of oedometer tests in which the samples were first loaded under natural water content conditions, avoiding evaporation, to a vertical stress equivalent to the overburden load. Then, specimens were soaked and deformations recorded. Tests were continued, under saturated conditions as indicated in Fig. 4. Measured deformations upon wetting have been plotted in Fig. 5 against the confining vertical load during saturation. The scatter of results is explained by the different initial porosity (or dry density) of samples. In order to define a simple criteria two tentative lines have been plotted in Fig. 5. One (γ_d = 1.7 T/m^3) may represent relatively low compaction density whereas the other (γ_d = 1.9 T/m^3) corresponds to good compaction conditions. The results indicate that a relatively

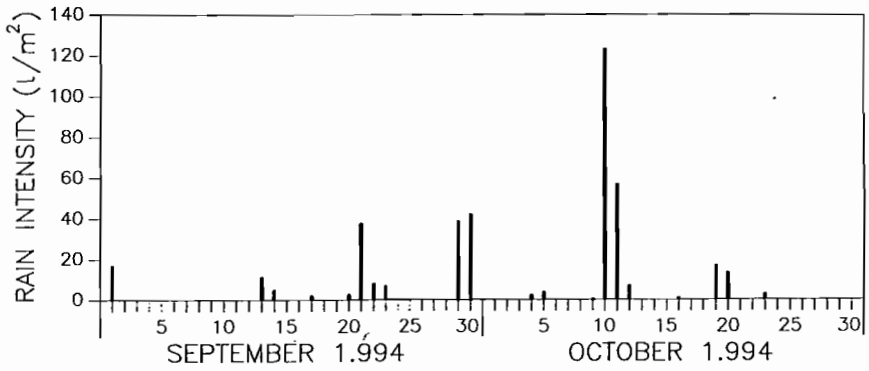

Fig. 1 – Rainfall distribution.
Fig. 1 – Distribuzione delle piogge.

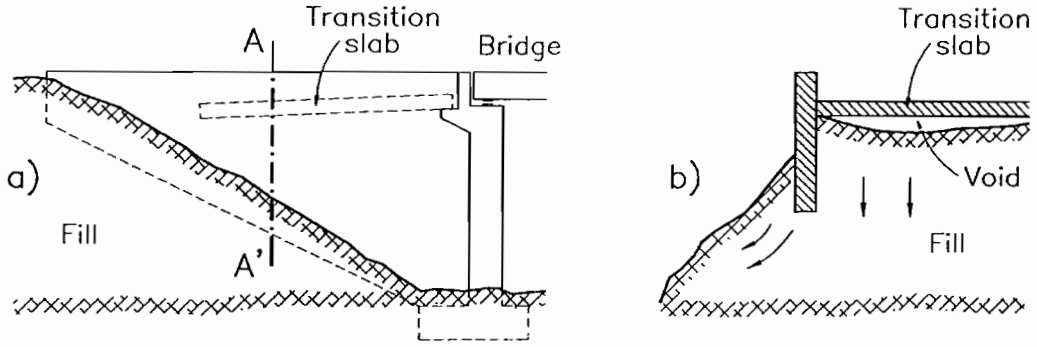

Fig. 2 – Scheme showing the nature of voids below transition slabs in bridge abutments. a) Side view. b) Cross section AA'.
Fig. 2 – Tipologia dei vuoti formatisi in corrispondenza delle spalle. a) sezione longitudinale. b) sezione trasversale.

small collapse strain potential, increasing with confining stress, still remains in the fills.

2.3. *Strength tests*

The results of conventional direct shear tests performed on three samples, once saturated, are summarized in Table 1. The "worst case" is represented by S4 M17, residual value ($c' = 0$, $\varphi' = 27.6°$).

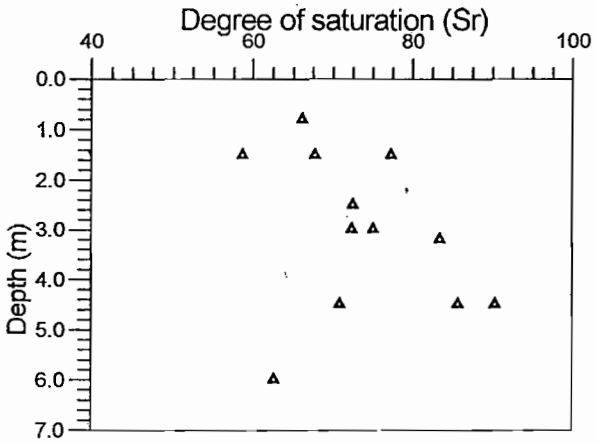

Fig. 3 – Degree of saturation, measured in samples, after heavy rainfall.
Fig. 3 – Grado di saturazione misurato su campioni prelevati dopo piogge intense.

Suction controlled tests were also carried out in the Escario shear box [ESCARIO, 1986]. The results obtained in two testing programs on specimens from samples S4 M17 and S2 M7 are plotted in Figs. 6 and 7 respectively.

Individual tests were made in stages imposing first a given net vertical stress and suction, shearing the specimen to the verge of failure and changing net vertical stress and suction to the next testing point. Shear strength envelopes for saturated specimens are plotted in Figs. 6 and 7 for reference. The number of data points is limited but they clearly show a fast increase in apparent cohesion with suction. For low values of suction the rate of increase in strength with suction is controlled by the φ' angle (note in particular Fig. 6) in a manner consistent with the effective stress principle for a (quasi) saturated material.

Tab. I – Conventional direct shear tests on saturated samples.
Tab. I – Prove di taglio diretto su campioni saturi.

Sample	*c' (MPa)*	*φ' (°)*	*Remarks*
S2 M7	0.03	21°	Peak value
S4 M17	0	29.4°	Peak value
S4 M17	0	27.6°	Residual value

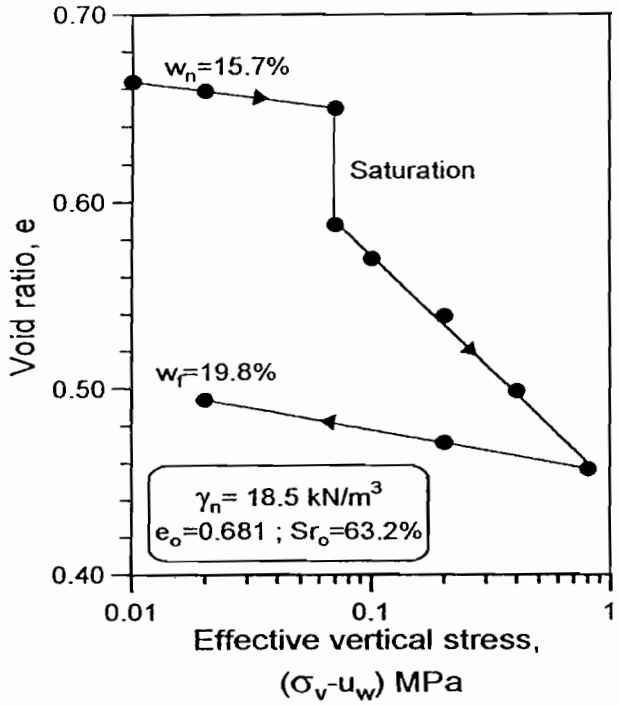

Fig. 4 – Oedometer test showing collapse upon saturation.
Fig. 4 – Prove edometriche in cui si manifesta il collasso a seguito della saturazione.

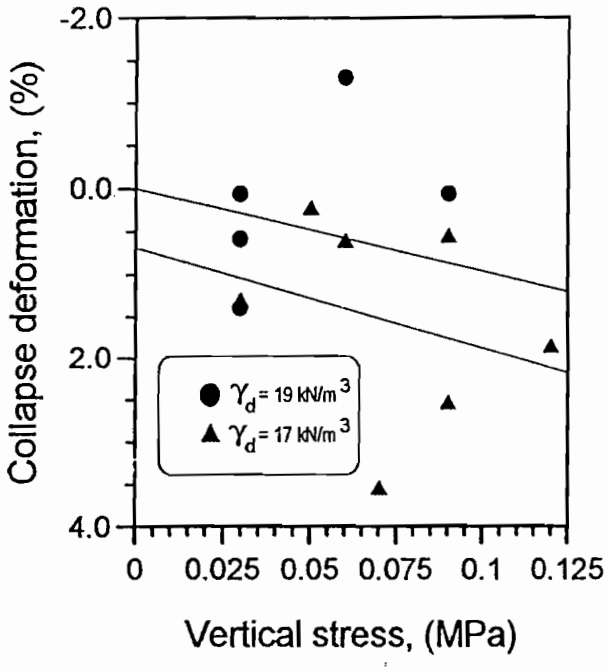

Fig. 5 – Variation of collapse strain with vertical stress and dry density.
Fig. 5 – Variazione della deformazione al collasso con la tensione verticale ed il peso dell'unità di volume del secco.

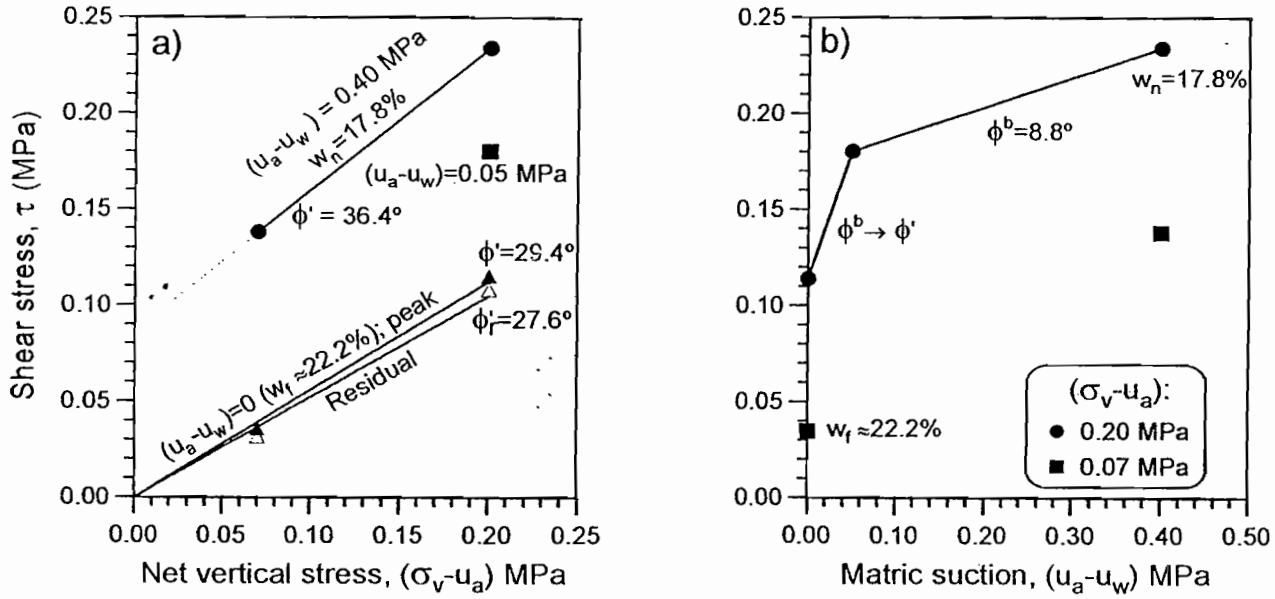

Fig. 6 – Suction controlled shear tests. a) Shear strength vs. net vertical stress. b) Shear strength vs. suction. Sample S4 M17.
Fig. 6 – Prove di taglio a suzione controllata. a) Resistenza al taglio in funzione della tensione normale (netta). b) Resistenza al taglio in funzione della suzione. Campione S4M7.

2.4. Other tests

Water retention characteristics, as determined in a suction controlled oedometer cell under a net confining vertical load σ_v = and decreasing suction are shown in Fig. 8 in terms of both degree of saturation and water content. Note that the plotted curve represents an inhibition phenomena which is the extreme condition whose effects are sought.

The consolidation stage of the saturated direct shear tests was useful to determine a few consolidation parameters and in particular the specimen permeability. Measured values ranged between $k = 1.4 \cdot 10^{-7}$ cm/s to $4 \cdot 10^{-9}$ cm/s. Most likely the relevant "in situ" permeability is closer to the higher

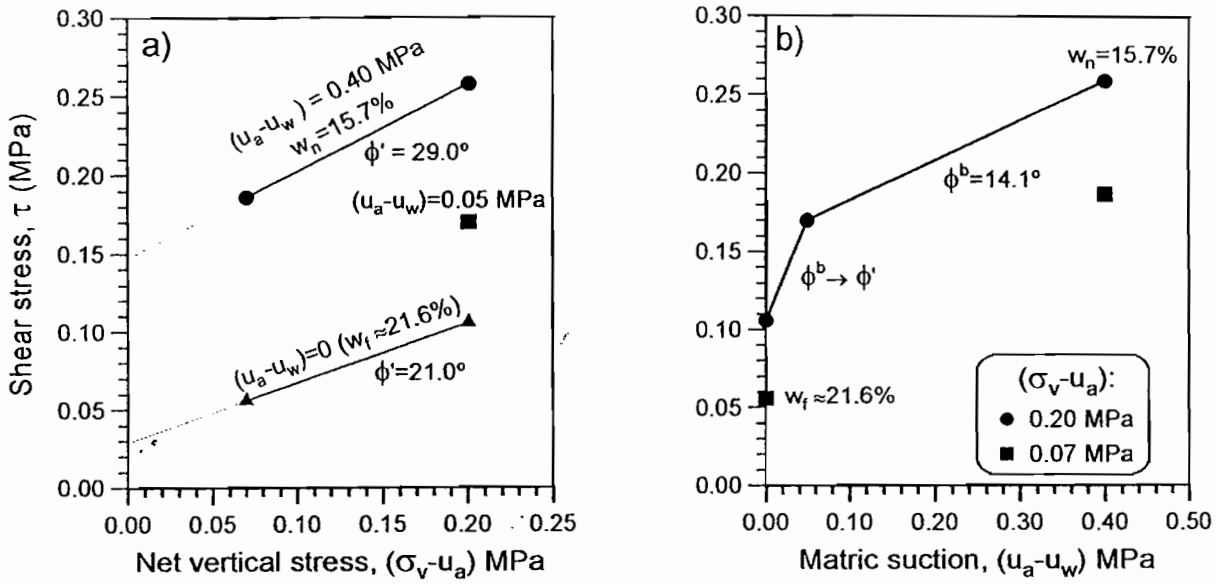

Fig. 7 – Suction controlled shear tests. a) Shear strength vs. net vertical stress. b) Shear strength vs. suction. Sample S2 M7.
Fig. 7 – Prove di taglio a suzione controllata. a) Resistenza al taglio in funzione della tensione normale (netta). b) Resistenza al taglio in funzione della suzione. Campione S2M7.

measured values due to soil heterogeneity at different scales.

3. Behaviour during further infiltration

3.1. Slope stability

Since the fills maintained a significant suction after a heavy rainfall event and this suction is able to confer an important apparent cohesion to the soil, the issue for the assessment of future sliding risk is to determine if future intense rains may reduce further the existing suction. In order to analyze this situation 2D infiltration analysis has been carried out with the help of NOSAT computer code. NOSAT solves coupled hydromechanical problems in unsaturated soils and has been described in ALONSO *et al* [1988]. The solved case is represented in Fig. 9. The embankment analyzed has a 7m height and the slope is 33.7°. A uniform initial suction s_i =0.5 MPa was adopted in view of measured water contents in samples and the water retention curve determined (Fig. 8).

Rain was assumed to act on the unprotected slope and shoulder. A concentrated water intake was also assumed at the curb-pavement contact where a longitudinal crack had developed. The saturated permeability was taken as $K_{ws} = 5 \cdot 10^{-7}$ cm/s which is the highest value measured in the laboratory. The variation of water permeability with suction and the water retention curve are indicated in Table II.

The evolution of water pressure at mid height in a point relatively close (1m) to the surface, if a non-

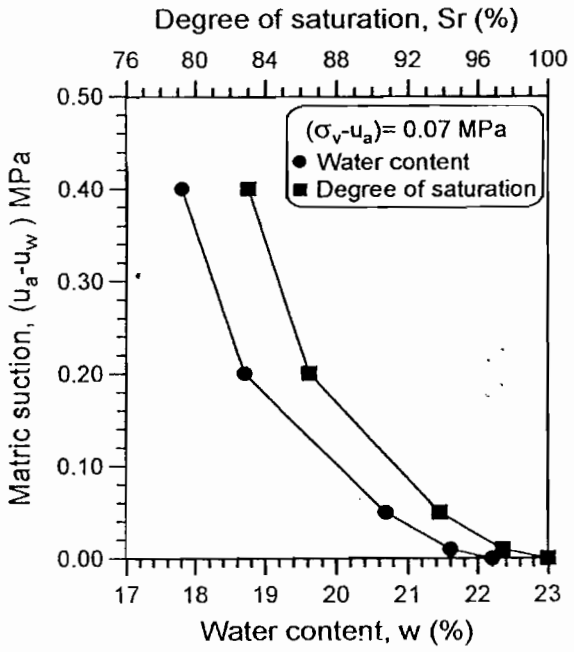

Fig. 8 – Water retention curve.
Fig. 8 – Curve di ritenzione dell'acqua.

stopping rain is assumed to fall on the slope, is shown in Fig. 10. It is observed that after 10 days of rain a suction s = 0.1 MPa is still in place. The reduction in suction with time is a slow process (note the logarithmic scale of the graph). Fig. 11 shows the suction distribution in the slope after ten days of rainfall. Only a narrow surficial layer (0.5m in thickness) seems to be close to saturation. The fill will therefore maintain a relatively high cohesion which is very effective in preventing instabilities. This is illustrated in Fig. 12 which indicates the critical slip

Tab. II – Parameters for the coupled flow-deformation analysis.
Tab. II – Parametri dell'analisi accoppiata.

Property	*Expression*	*Parameters*
Water permeability	$K_w = K_{ws}\left(\frac{S_r - 0.25}{0.75}\right)^3$	$K_{ws} = 5 \cdot 10^{-7}$ cm/s
Retention curve	$S_r = S_{ro} - (1 - e^{-as})b$ (s = suction in Pa)	$S_{ro} = 0.975$ $a = 0.6955 \cdot 10^{-6}$ Pa^{-1} $b = 0.7$
Volumetric deformation	$\Delta e = a\Delta(\sigma - p_a) + b\Delta s + c\Delta(\sigma - p_a)\,\Delta s$ σ = Average stress (Pa) p_a = Air pressure (Pa)	$a = -0.136 \cdot 10^{-5}$ Pa^{-1} $b = 0.2 \cdot 10^{-7}$ Pa^{-1} $c = -0.4 \cdot 10^{-12}$ Pa^{-2}
Poisson coefficient	v	$v = 0.33$

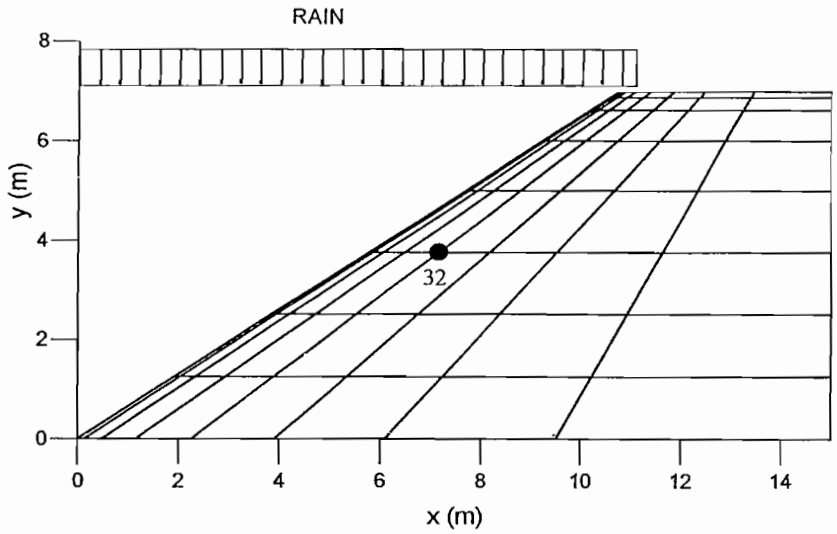

Fig. 9 – Model for infiltration analysis of the road embankment.
Fig. 9 – Modello per analisi di infiltrazione nel rilevato stradale.

circles and the minimum safety factor (F=1.8) for a uniform cohesion of 0.01MPa which is certainly a very low value in view of results obtained in suction controlled shear tests. It is concluded that the risk of slope instability is very small with the exception of very shallow slab type of slides which may affect the vegetation cover.

3.2. Deformations

A second important question for the future behaviour of the fills concerns the possibility and intensity of further deformations in the case of repeated heavy rainfalls. To investigate this possibility a coupled flow-deformation analysis has been performed using NOSAT. Suction induced deformations are introduced in NOSAT by means of state surfaces which define the collapse or swelling strains as a function of net mean stress and suction changes. Based on the collapse data presented in Fig. 5 the state surface defined in Tab. II was used for computations. This state surface provides also data for the determination of the bulk modulus of deformation.

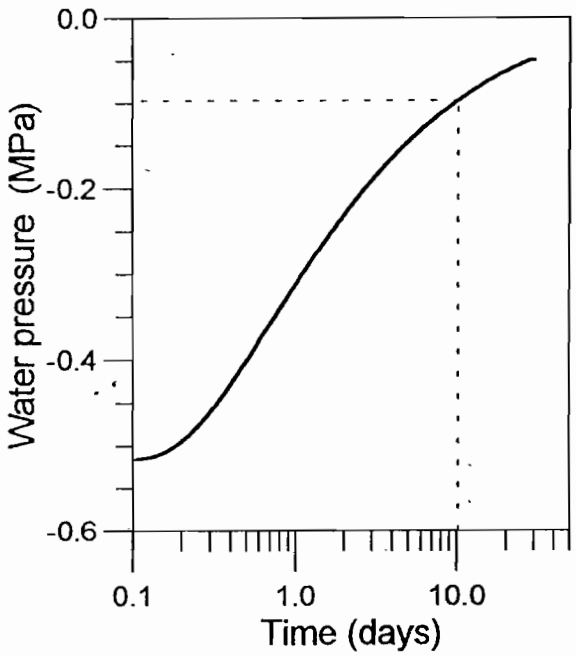

Fig. 10 – Evolution of water pressure in node 32 (see Fig. 9).
Fig. 10 – Evoluzione della pressione interstiziale nel nodo 32 (vedi fig. 9).

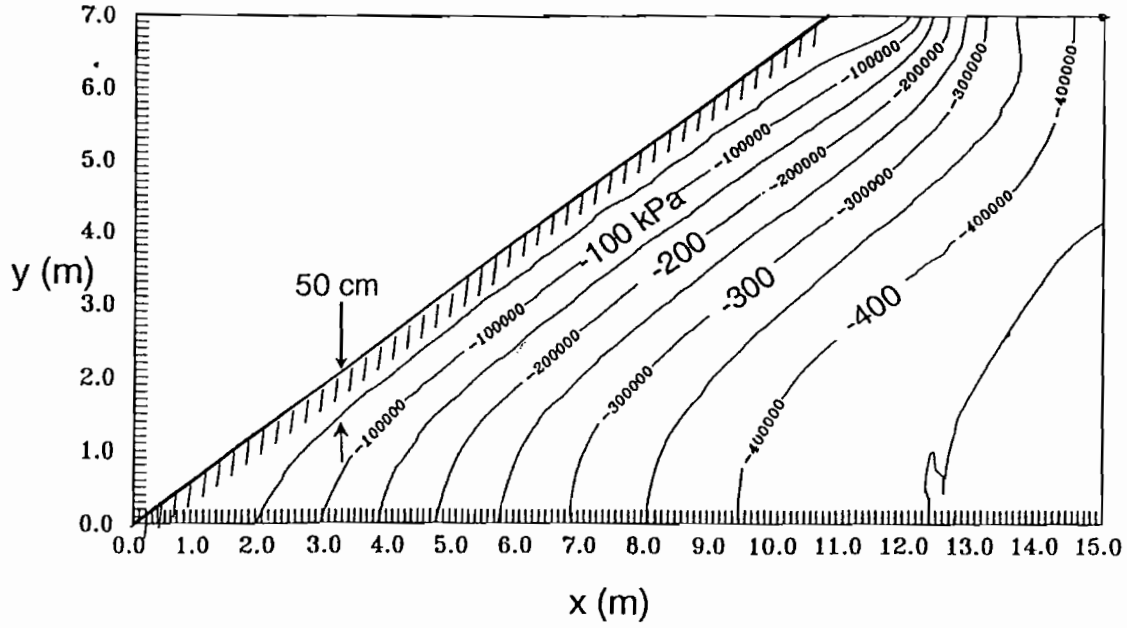

Fig. 11 – Suction distribution after ten days of rainfall.
Fig. 11 – Distribuzione della suzione dopo dieci giorni di pioggia.

A constant Poisson coefficient $v = 0.33$ was also adopted.

The experimentally determined water retention curve was defined by means of the exponential function (Fig. 8) given in Table II. Finally, the variation of water permeability with degree of saturation was approximated by means of an equation initially proposed by IRMAY [1954] and widely adopted in unsaturated flow studies. An interesting result of the analysis is the computed pattern of fill deformations as shown in Fig. 13, which corresponds to a rain period of 21 days. The embankment tends to shrink in a isotropic manner. This is a consequence of the assumption that collapse deformations are essentially volumetric. This is only a first approximation but visual inspection in the field indicated that wide vertical openings developed at the contact between fill and the vertical walls of bridge abutments. Horizontal displacements were estimated to be of the same order of magnitude of vertical settlements. For 5-7m high fills these collapse induced settlements and horizontal displacements could reach 20-30cm.

The remaining deformation potential is, however, much smaller. This is illustrated in Fig. 14 which shows the evolution of settlement of the crest of the fill as a function of time for a continuous rain. The two curves plotted correspond to a relatively compact (γ_d = 1.9 gr/cm^3) or loose (γ_d = 1.7 gr/cm^3) fill as it was defined in Fig. 5. For a 10 day rain the loose fill may experience a settlement close to 1cm. The dense fill does not experience any relevant displacement during the same period.

In order to cover the different fill heights it is convenient to plot the settlement evolution in dimensionless terms. This is shown in Fig. 15 where the normalized settlement (settlement at time t divided by the final ($t \to \infty$) settlement is plotted against the dimensionless time $T = t \cdot K_{ws}/H$ where H is the slope height and K_{ws} the fill saturated permeability.

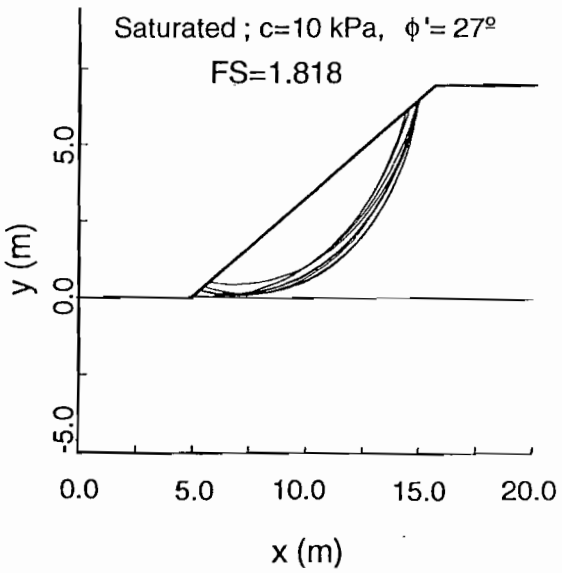

Fig. 12 – Stability analysis for $c' = 1$t/m^2 and $\varphi' = 27°$.
Fig. 12 – Analisi di stabilità per $c' = 1$t/m^2 e $\varphi' = 27°$.

Deformations follow changes in water content in the fill. For the times t_2 and t_3 , indicated in Fig. 15, the computed distribution of degree of saturation within the slope are given in Fig. 16. The logarithmic time scale in Fig. 15 indicates that the saturation process is slow. It was concluded that even under extreme rainfall events it would be unlikely for the highest fills to reach settlements (and horizontal deformations) in excess of 1.5 cm.

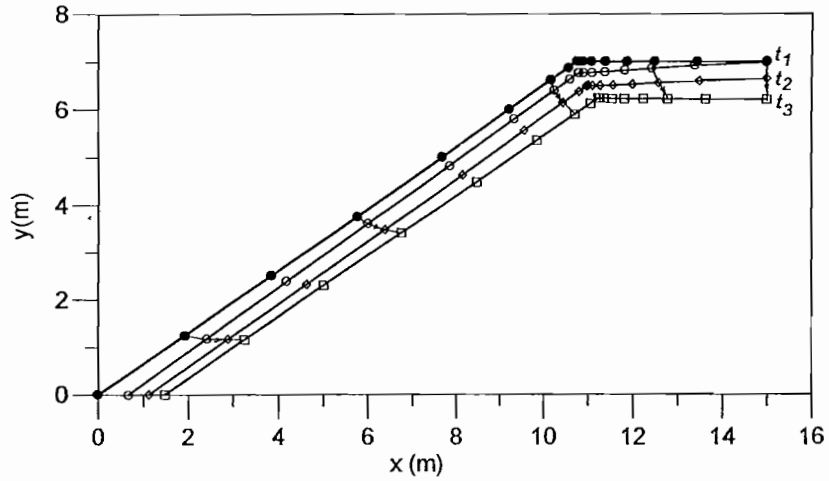

Fig. 13 – Pattern of rain induced settlements at t = 21 days.
Fig. 13 – Distribuzione dei cedimenti prodotti dalle piogge dopo 21 giorni.

4. Discussion and conclusions

Heavy rainfalls on a number of recently built road fills induced several damage features which could be attributed to three different phenomena: slope erosion, shallow slides and fill collapse. The latter was a widespread phenomena and led to maximum settlements and horizontal deformations in the range 20-30cm.

As a consequence, portions of the pavement became unsupported, several light foundations lost stability and important voids developed between fill and bridge abutments. The most serious defect was, however, the loss of support experienced by several transition slabs between bridge abutments and embankments which led to extensive repairs. The design of the lateral wing walls of the bridge abutments did not provide a convenient lateral confinement to limit the fill settlement. Both shallow sliding and fill collapse contributed to the loss of support of the slabs.

The main reason for the collapse experienced by the fill was the dry-of-optimum field compaction conditions. On average, water content was 3% to 5% lower than Normal Proctor optimum. Dry density was also somewhat lower than optimum.

It was shown, both by direct field observations and modelling of the process of rain infiltration and associated soil collapse, that fills tend to deform both vertically and horizontally in an isotropic way.

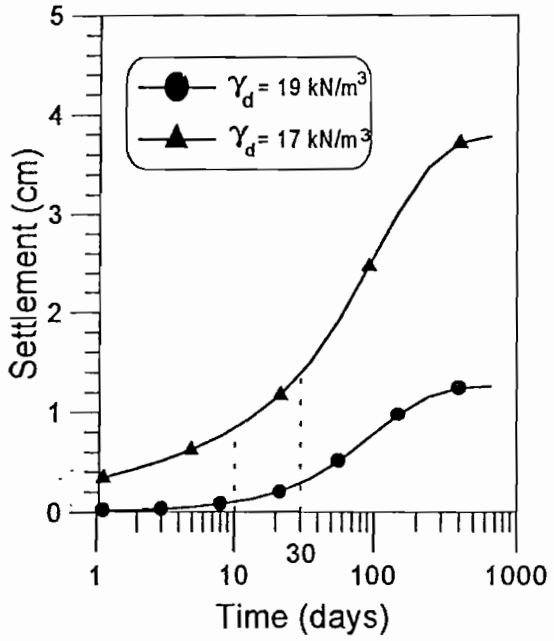

Fig. 14 – Settlement of the crest of a 7m high fill.
Fig. 14 – Cedimenti alla sommità di un rilevato alto 7 m.

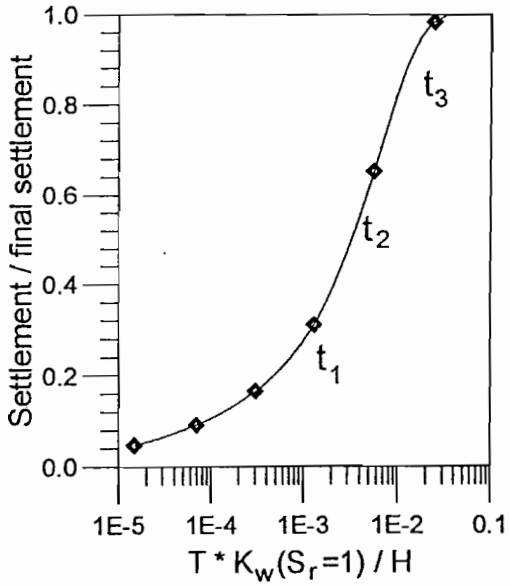

Fig. 15 – Dimensionless plot showing the evolution of normalized fill crest settlement.
Fig. 15 – Evoluzione del cedimento normalizzato alla sommità del rilevato.

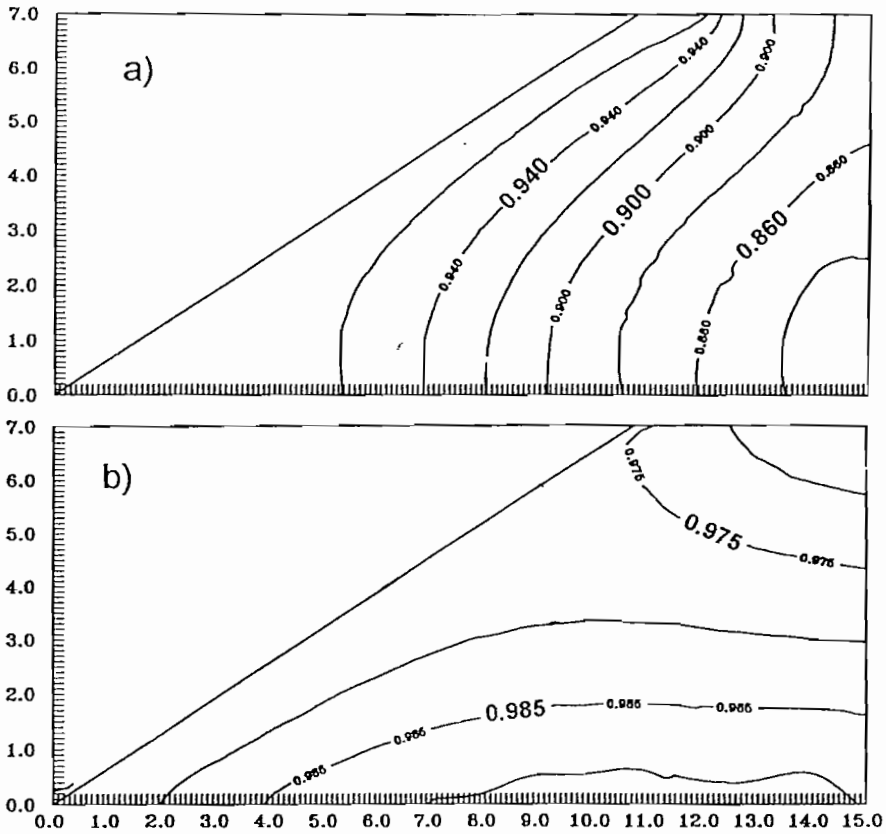

Fig. 16 – Distribution of degree of saturation for times t_2 and t_3 (see Fig.15).
Fig. 16 – Distribuzione del grado di saturazione ai tempi t_2 e t_3.

This is consistent with the volumetric nature of soil collapse.

Sliding was observed only in low density fills when they reached saturation. In general, only shallow slides were observed. The analysis shows that deep seated instabilities are extremely unlikely because of the apparent cohesion provided by suction and the nature of the saturation phenomenon which is a slow process governed by soil permeability and boundary conditions. The impervious pavement contributes to retard the saturation of the fill core even under extreme rainfall events.

Soak-under-load oedometer tests on recovered samples after the rainfalls showed that the remaining collapse potential was relatively small (1% to 2%, depending on the average dry density). The remaining settlement potential in case of repeated heavy rainfalls seems to be small due to the retarded naure of the infiltration process. The maximum residual settlement for the largest fill was estimated in 1.5cm.

Suction controlled direct shear tests has shown that a suction of 0.4MPa, a value which may remain essentially unchanged within the fills, provides an apparent fill cohesion in the range 0.09-0.15MPa. These high values explain the low risk of deep seated failures in the fills.

References

ALONSO E.E., BATLLE F., GENS A. and LLORET A. (1988) – *Consolidation analysis of partially saturated soils. Application to earthdam construction.* Numerical Methods in Geomechanics, G. Swoboda ed., Innsbruck, pp. 1303-1308.

ESCARIO V. and SAEZ J. (1986) – *The shear strength of partly saturated soils.* Géotechnique, *36*, pp. 453-456.

IRMAY S. (1954) – *On the hydraulic conductivity of unsaturated soils.* Trans. Amer. Geophys. Union, 35, pp. 463-468.

Deformazioni di un rilevato stradale indotte dalla pioggia

Sommario

Questo lavoro descrive i fenomeni di erosione, di instabilità superficiale e di collasso di rilevati stradali indotti da eventi piovosi di una certa entità. Sono state realizzate prove edometriche e prove di taglio a suzione controllata su campioni prelevati da sondaggi. È stata condotta un'analisi accoppiata filtrazione-deformazione in condizioni di parziale saturazione allo scopo di valutare il rischio di futuri fenomeni di rottura ed il potenziale residuo di collasso dei terreni di riempimento per effetto di eventi piovosi di una certa entità.